UNIVERSITÉ DE LIÈGE
BELSPO

DEPARTEMENT DE PHYSIQUE

Physique Theorique des Matériaux

REPORT

POSTDOC 2011-2012

Responsable:
Prof. Philippe GHOSEZ

Candidate:
Dr. Srijan Kumar SAHA

---

28 September 2012

Contents

Preamble

In this brief report, I present the results I have obtained during my POSTDOC at the University of Liège. My contract started on the 1^{st} of April, 2011 and I worked on the 'BELSPO' project (Structural phase transitions at finite temperature) within the group of Theoretical Physics of Materials at the University of Liège until the end of September 2012.

During the 18 months of POSTDOC, I have worked exclusively on the dynamical properties and the structural phase transitions at finite temperature. In the first part of this report, I present the results and the concluding remarks regarding the finite temperature effects on phonon dispersions and stability of the functional materials under study. The results obtained are going to be published. This project work has allowed me to become familiar with the SCAILD method.

In parallel to methodologic developments, the ferroelectric properties of different perovskites were also studied. Structural, electronic and vibrational properties of chloride-based perovskites are described in the second part of this report.

A summary of my scientific output is presented in the last part. This last part includes a list which shows that during the period of POSTDOC, I have attended various meetings and workshops and delivered various presentations with BELSPO support properly advertised. This part also provides a list of publications in preparation within BELSPO support.

Structural phase transitions at finite temperature

The aims of the present project were (i) to develop a systematic and powerful theoretical approach based on density functional theory (DFT) to predict the structural phase transitions at finite temperature (specially T_c) and (ii) to take advantage of this tool for designing, in collaboration with experimentalists, oxide ultra-thin films and superlattices with optimized ferroelectric properties.

1 Motivation and objectives

First-principles simulations based on density functional theory (DFT) have been proved to be particularly useful to help understanding how to tune the ferroelectric properties and the competition between structural instabilities in various types of oxides[1, 2]. In such calculations, the appearance of a ferroelectric instability is tracked from the appearance of an unstable polar phonon mode. Although such calculations are valuable to determine whether the ground-state is ferroelectric or not, they are performed at zero Kelvin and do not give any quantitative information about the phase transition temperature, Tc, which is nevertheless a key information to be provided to the experimentalists.

Conventional methods to calculate the thermodynamical properties of crystals use the harmonic phonon spectra and hence, do not work in the case where the studied crystal structure exhibits unstable phonon modes at zero Kelvin; this is, for instance, the case in the high temperature body-centered cubic (bcc) phase of many metals or the high-temperature phases of ferroelectric compounds. To bypass this limitation, first-principles based effective Hamiltonians were successfully developed to access the finite temperature of ferroelectrics but building such a model is not straightforward since it requires to identify the relevant structural degrees of freedom and also includes a lot of approximations in the treatment of anharmonicities. Recently, Souvatzis[3] proposed an original method for calculating temperature dependent phonon spectra self-consistently from first principles, providing access to T_c. The method was successfully applied to simple systems such as metals and also

to ZrO2 but without explicit treatment of the long-range interatomic interactions.

The objective of the present project is to generalize the method of Souvatzis et al. to deal ferroelectric systems properly and to explore the capability of this approach to be helpful in the design of ferroelectric nanostructures.

2 Methodology

We use recently developed SCAILD method in order to describe structural transition at finite temperature. To include the effects of phonon-phonon interactions on the phonon frequencies at elevated temperatures, in this method, one displaces the atoms simultaneously in a supercell based on all phonons with wavevectors $\mathbf{q}$ found to be commensurate with the supercell, and displacements can be written as

$$\mathbf{U_R} = \frac{1}{\sqrt{N}} \sum_{\mathbf{q},s} \mathcal{A}_{\mathbf{q}s} \epsilon_{\mathbf{q}s} e^{i\mathbf{qR}} \qquad \text{Eqn.(a)}$$

where $\epsilon_{\mathbf{q}s}$ are the phonon eigenvectors and

$$\mathcal{A}_{\mathbf{q}s} = \pm\sqrt{\frac{\langle \mathcal{Q}_{\mathbf{q}s} \mathcal{Q}_{-\mathbf{q}s} \rangle}{M}} = \pm\sqrt{\frac{\hbar}{M\omega_{\mathbf{q}s}} \Big[\frac{1}{2} + n\Big(\frac{\hbar\omega_{\mathbf{q}s}}{k_B T}\Big)\Big]},$$

when $n(x) = 1/(e^x - 1)$ is the Bose function, M is the mass of atoms, and $\mathcal{Q}_{\mathbf{q}s}$ are the canonical phonon operators. A first principles calculation provides the Hellman-Feynman forces acting on the displaced atoms, and a new set of phonon frequencies are obtained from the Fourier transform $\mathbf{F_q}$ of the forces,

$$\bar{\omega}_{\mathbf{q}s} = \Big[\frac{\epsilon_{\mathbf{q}s} \cdot \mathbf{F_q}}{\mathcal{A}_{\mathbf{q}s} M}\Big]^{1/2} \qquad \text{Eqn.(b)}$$

The simultaneous presence of several frozen phonons in the supercell introduces geometric disorder, that is, entropy, which in turn renormalizes the phonon frequencies. This method which obtains the frequencies based on the calculated Hellman-Feynman forces by projecting out each mode's restoring force, relies on an iterative scheme to obtain a self-consistent phonon spectrum.

In the SCAILD scheme, the finite-temperature frequency distributions can be obtained despite the absence of any explicit time dependence by virtue of the stochastic damping and the ergodic principle. This is realized by choosing the magnitude of the frozen phonon amplitudes in a way that they reproduce the atomic mean square displacements dictated by thermodynamics, and by the re-randomization of the frozen phonon phases at each new SCAILD iteration, here represented by the randomization of the $\pm$ signs of the amplitudes. Thus, in this method, the amplitudes of displacements depend on temperature and the phonon frequencies. Fig. 1

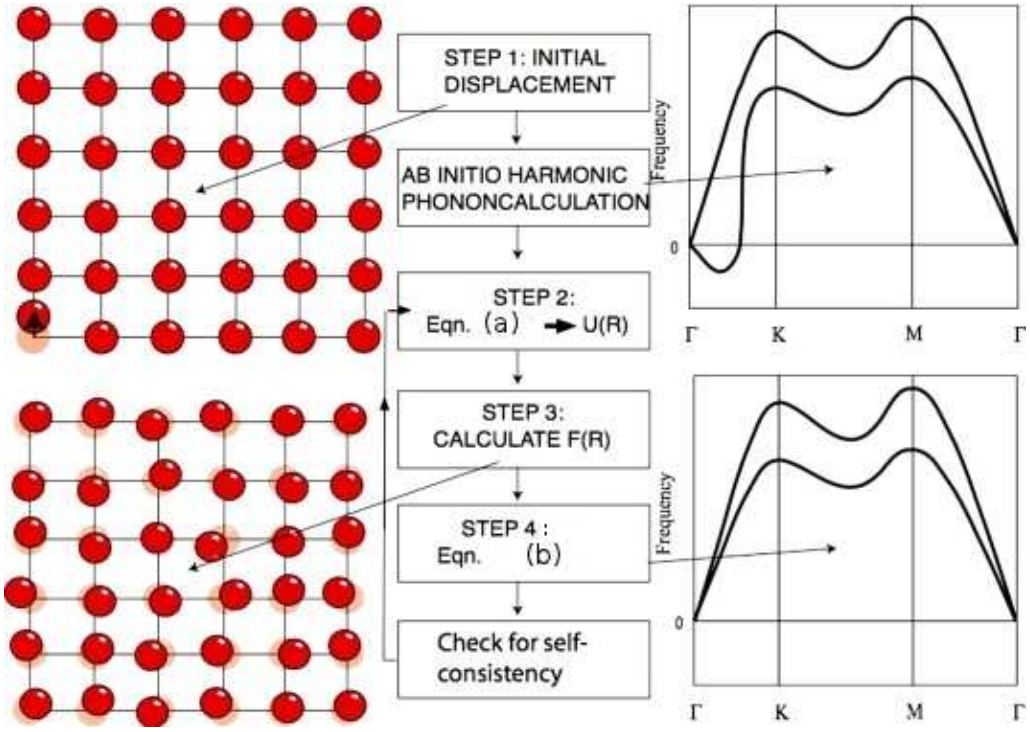

Figure 1: Schematic outline of the steps involved in a SCAILD calculation.

schematically outlines the different steps performed in a SCAILD calculation. This is a method that takes into account phonon-phonon interaction up to infinite order by combining first principles calculations of inter atomic forces with a mean field formulation of the lattice dynamics which can be seen as the phonon equivalent of the Hartree-Fock approximation.

3 Some technical issues and my contribution to coding

The SCAILD is a newly developed code and its applications are hitherto limited to the systems with one, two or a very few atoms per primitive cell (such as Ti, Zr, NiTi to name a few). However, for a complex system, like $BaTiO_3$ there is no study reported yet. The reason lies in the fact that for a large number of atoms per primitive cell, the simultaneous displacements of atoms in the supercell with increasing temperature gives forces so arbitrary that it becomes difficult to reach proper convergence in the iterations for the self-consistent cycle. Sometime after various iterations phonon dispersions converge to totally wrong values. We also find that for a complex system with a low symmetry or a large number of atoms, the acoustic

sum rule (ASR) becomes violated. I have fixed this problem by implementing a different ASR enforcement trick inside SCAILD code. My contribution in fact makes sure that the ASR will be respected even when a system does not have a simple structure with simple cubic symmetry. We check that the my new ASR enforcement works pretty well also for complex systems, for instance, for tetragonal (I4/amd) or cmmm phase of calcium.

The SCAILD code originally was interfaced with the VASP package which is not a free software. It is indeed a good idea to extend the use of SCAILD method with other freely available softwares like ABINIT or Quantum Espresso. This method is being implemented in the ABINIT international software package (www.abinit.org) where the group ϕ-TheMa contributes to develop since many years and which is particularly suited for phonon calculations. In order to benchmark this on-going development, I interface the SCAILD code with the ABINIT and Quantum-Espresso packages.

4 Results and Discussions

4.1 Successful application of SCAILD on Calcium

Calcium is the lightest element in the alkaline-earth metals group. Like other elements in this group, structural phase transitions are observed under increasing pressure. Nevertheless, the global behavior of the transitions is still not fully understood. Ab-inito DFT calculations have been applied in recent years to describe the high-pressure structure for Calcium, but many discrepancies with the experimental results are found. In this work, we try to solve these discrepancies by incorporating the finite temperature effects.

At ambient pressure and temperature, Ca presents a face centered cubic (fcc) structure, which transforms into body centered cubic (bcc) at 20 GPa, then into simple cubic (sc) at 32 GPa and finally to an unknown phase at 42GPa[4]. As the pressure increases, a volume reduction together with a decreasing coordination number (fcc (12)$\rightarrow$ bcc (8) $\rightarrow$ sc (6)) is observed. This counterintuitive behavior is due to Calcium's band structure, which allows a $4s \rightarrow 3d$ electron transfer under increasing pressure.

So far, standard (harmonic) ab-initio DFT calculations are attempted to predict these structures, but they fail in describing correctly the high pressure behavior. In particular, the unknown phase of calcium, which exists in the pressure range 33-119 GPa, is not predicted to be sc (the structure confirmed by all the experimental papers: [4, 8]) and other phases are predict to be thermodynamically more stable. Moreover, the sc phase is also found to be dynamically unstable in the above pressure range, and phonon analysis presents imaginary frequencies [9]. A big debate is still

open and many possibilities have been investigated to determine the real structure of the high-pressure calcium phases, with many different methods. The ergodic convergence of molecular dynamics studies are difficult to assess, and some explicitly anharmonic methods only include lower (third and fourth) order anharmonicities [10]. Other possibilities have been investigated to determine the real structure of the high-pressure calcium phases using genetic algorithms, quasirandom methods and classical elastic constants calculations.

Our calculations show that sc gets stable between 30 and 35GPa while it become unstable again between 45 and 50GPa, as is evident from Fig.3. Thus, even taking into account anharmonic effects, sc phase become stable only in a limited pressure range of about 10GPa, between 35 and 45 GPa.

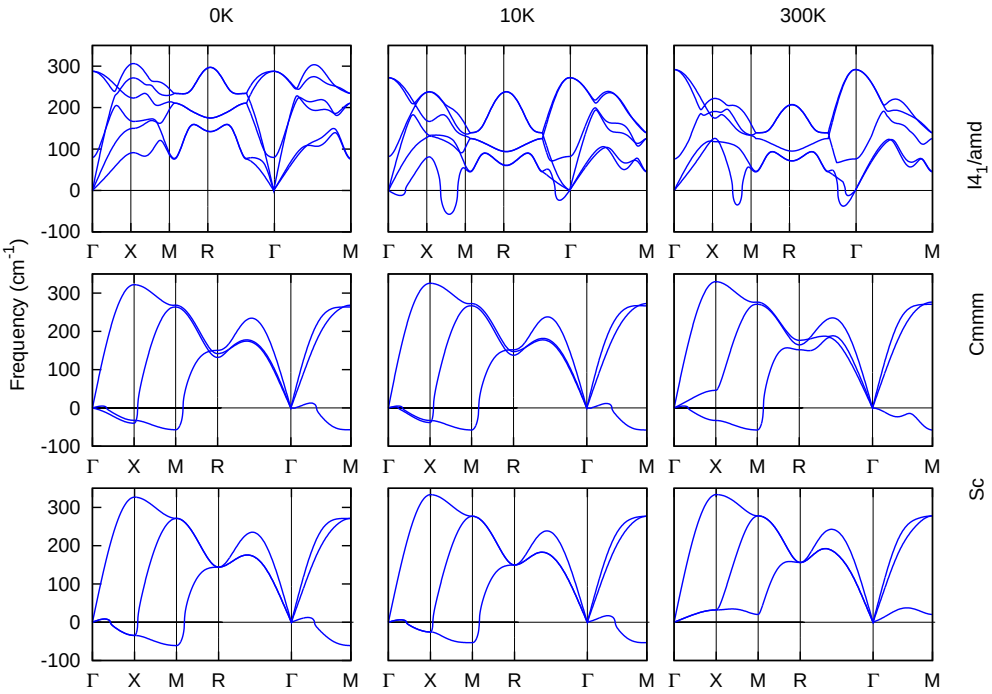

Figure 2: Anharmonic phonon dispersion curves for the sc phase: at P=0 GPa sc is dynamically unstable, at P=35GPa is stable at room temperature and unstable at low temperature while at high pressure (70 GPa) is stable for low and high temperature

We have studied five phases: the face centered cubic (fcc) which is thermodynamically stable until 20 GPa, the body-centered cubic (bcc) stable until 33 GPa, the simple cubic (sc), the tetragonal $I4_1/amd$ phase and the orthorombic $Cmmm$ phase discovered by Mao [6]). We compare in particular the sc, $Cmmm$ and $I4_1/amd$ which are possible candidates for the unknown phase. We explicitly consider two con-

tributions: first we calculated the Gibbs free energy adding independently electronics and phononics contributions. We conclude that entropy corrections are not enough to explain the errors in the phase diagram. Second, we explicitly computed the anharmonic contributions due to the finite temperature by using SCAILD method [3]. Our analysis revealed that anharmonic contributions can contribute in different way to the stability of the different studied phases. It can contribute to stabilize a phase (as in the case of sc phase, which is stable for 40GPa at room temperature) but they can also de-stabilize the phonon vibrational spectra at finite temperature, as for $I4_1/amd$ or they can leave it unvaried as for $Cmmm$. This supports the idea that a low temperature phase with a slightly distorted sc structure, different both from $Cmmm$ and $I4_1/amd$ could exists in the 32-109GPa range[6] which seems to be Cmmm due to dynamical fluctuation, and transforms to the observed sc structure somewhere in the 0-300K temperature range. This contrasts the results found by Errea *et al.*[10] who argued that strong quantum anharmonic effects make the imaginary phonons frequencies positive even at zero temperature for P=50GPa.

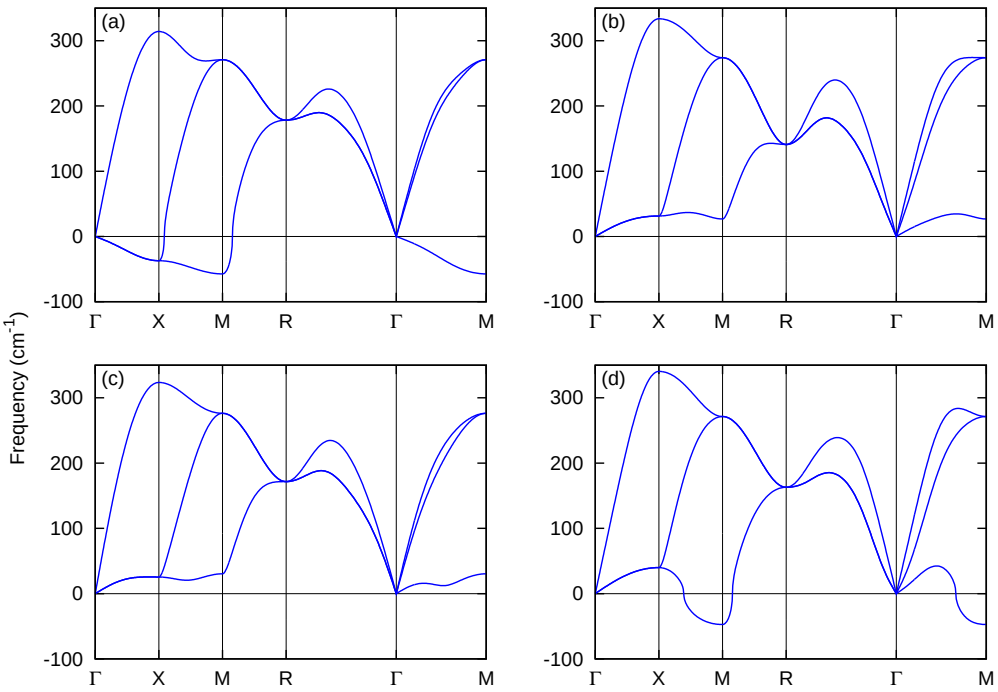

Figure 3: Phonon dispersion curves including anharmonic terms for sc phases at 300K and (a) 30 GPa , (b) 35 GPa, (c) 45 GPa and 50 GPa.

In Fig.4, self-consistent temperature-dependent phonon spectra are shown for the three phases which are possible candidates: the $I4_1/amd$ tetragonal phase, the orthorombic Cmmm and the simple cubic phase at different values of temperature

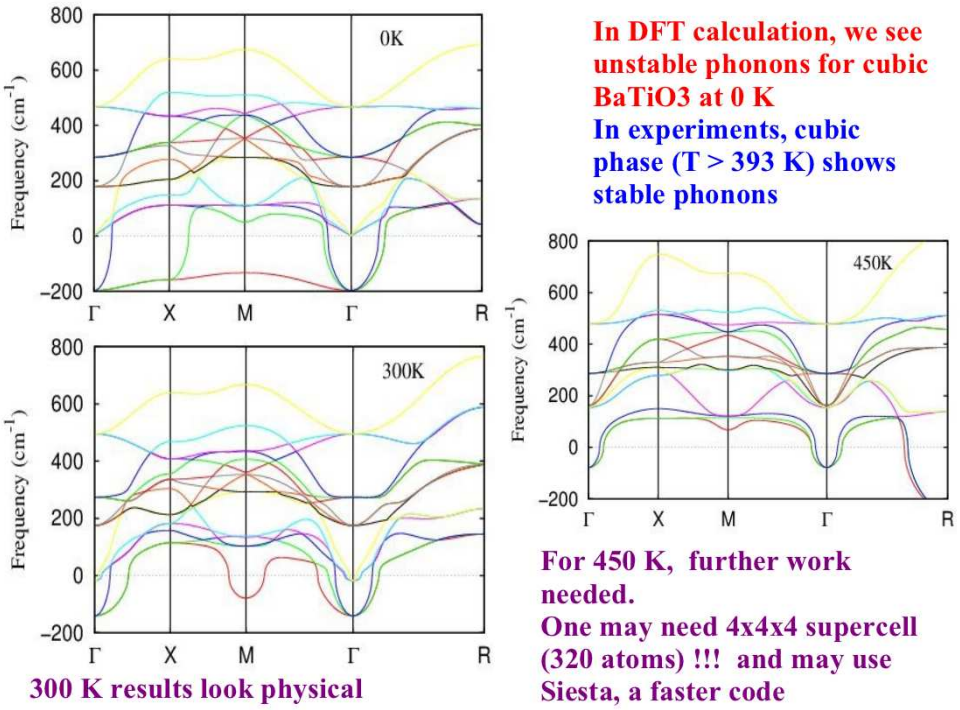

Figure 4: Anharmonic stabilization of BaTiO3 with increasing temperatures

for 40GPa. For these calculations, we use a 4x4x4 supercell, with 4^3 k-point mesh. We find that the sc phase get stable at high temperature (as shown previously by Tse *et al.* in [7]). This result is in strong contrast with the self-consistent harmonic approximation SCHA which gives stable modes for high pressures even at 0K as a result of quantum fluctuations[10]. By using the SCAILD method instead of the SCHA method all the terms (infinite in principle) in the perturbative expansion are considered instead of the former four as in [10]. These results confirm the result found by Yao *et al.*[11] and support the general idea that, between 32 and 109 GPa, a sc-distorted stable phase exists and transforms to sc somewhere in the 0-300K temperature range due to anharmonic effects.Anharmonic effect modify the other two phases studied in different manners. $I4_1/amd$ is the only stable phase at 0K (which corresponds to the harmonic calculation) but it becomes unstable as temperature increases at 10K, with imaginary modes close to the Γ point and between the M and R directions. Anharmonic contributions leave the vibrational spectra basically unvaried for the Cmmm case, it is in fact never stable in the Pressure range analyzed and even for the condition proposed in [7] (44GPa and 4K). Its stability range is probably really narrow in the phase space. In Fig.4, self-consistent temperature-dependent phonon spectra are shown for the $I4_1/amd$, Cmmm and sc phases at different values of temperature and 40 GPa.

In conclusion, temperature effects do not have a unique effect on stability of solids. In fact, they can contribute to stabilize a phase, as in the case of sc calcium, contribute to de-stabilize a phase, as in the case of the tetragonal $I4_1/amd$ phase, or they can leave it unvaried as in the case of orthorombic Cmmm. Finally, about the stability of an exotic phase of calcium, we found a result that is in agreement with the first experimental result [4] which predicted the sc phase stable up to 42 GPa. In this context, the SCAILD method was very successful.

4.2 Anharmonic stabilization of BaTiO3 using SCAILD

Using SCAILD, we also investigate the anharmonic stabilization of $BaTiO_3$ with increasing temperature. Our results are summarized in Figure 4. The instability at zero Kelvin has been reduced when one goes to 300 Kelvin. However, when temperature increases further the simultaneous thermal vibrations of atoms make the system more difficult to converge. Figure 4 shows that at 450 Kelvin the ASR is also violated which was further fixed by implementing a different ASR enforcement trick inside the SCAILD code. The Figure 4 further shows that at 450 Kelvin the phonon dispersion curves near R point shows imaginary frequencies which can be an artifact resulting from the difficulties in convergence. And these difficulties can arise from various issues such as supercell size, strong phonon-phonon coupling, and intrinsic complexities in structural distortions. It should here be mentioned that similar spurious imaginary frequencies near R point are also noticed in the case of zero Kelvin. VASP has various electronic minimization algorithm such as Normal, VeryFast, Fast, Conjugate, All, Damped, Subrot, Eigenval, None, Nothing, Exact, Diag. The use of the default (Normal) option in the case of $BaTiO_3$ provides spurious imaginary phonon frequencies at and near R point of the Brillouin zone. By using other options like VeryFast or Fast this spurious instability is corrected. The reason of that is still unclear. Further work is necessary for this system in order to get a more complete understanding of the behaviour of phonons at elevated temperatures. This understanding, in turn, must help to give any quantitative information about the phase transition temperature, Tc, which is indeed a key information to be provided to the experimentalists.

In conclusion, no satisfactory results have been obtained yet on $BaTiO_3$ in spite of intensive effects. We were at first very surprised. But we went recently to Uppsala to present these results and discuss these with the developers of the SCAILD method and it appears that they are also facing the similar problems, not succeeding to get reliable results for $BaTiO_3$. At this stage it is not clear if it is a limitation of the method itself or a problem of implementation.

Structural, electronic & vibrational properties of chloro-perovskites

1 Motivation

Perovskites and related materials are of continuing interest as they display a wide range of fascinating properties that are of fundamental importance and technological relevance [12, 13, 14]. This range, for instance, includes large and tunable dielectric permitivity; piezo-, pyro-, ferro- and antiferro-electricity; ferroeleasticity, antiferrodistortivity, collossal magnetoresistance; charge, spin, orbital ordering; spin-dependent transport and superconductivity; many of which are exploited already in various technological applications for electronics, data storage or sensing.

Even though the members of the perovskite family are often based on the same simple cubic structure with the nominal composition ABX_3 (where A and B are cations, and X is anion), such a wide variety of functional properties stems from their chemical flexibility to accommodate majority of the elements in the periodic table and the complex correlation that cations play in certain coordinations with anions, depending on the chemical species involved. Being paragentically supple, perovskites readily evidence a great variety of structural instabilities from antiferrodistortive to ferroelectric and antiferroelectric. Many of their properties depend crucially on the details of the distortions associated with these instabilities. The majority of the perovskite compounds studied so far, which render enticing structural instabilities are oxides, but the perovskite structure is also known for the halides, sulfides, hydrides, cyanides , oxyfluorides and oxynitrides.

Goldschmidt's tolerance factors are often used to describe the formability or stability of the perovskite structure and to help in the analysis of property trends (see Table 1). A previous study investigating the formabilities of ABX_3 halide perovskites using the empirical structure map constructed by the tolerance factor and the octahedral factor has found that both the tolerance and octahedral factor are necessary but not sufficient condition for the formability of halide perovskites and

a lowest limit of the octahedral factor exists for their formation; and the results are consistent with the earlier report for ABO_3 oxide perovskites. At present, such halide-based systems however are not regnant to first-principles theoretical study as oxide-based systems are. So it is useful to carry out a systematic study to determine which of them are stable, which are unstable, and the nature of the instabilities, which will in turn provide useful clues for the exploration of new materirals. More specifically, one crucial subobjective is to determine whether some members of the family are the analogs of oxide perovskites in displaying ferroelectric or/and multiferroic behaviors. The origin of ferroelectricity is associated with structural phase transitions, where a symmetry breaking, specifically from a centrosymmetric to a noncentrosymmetric structure, occurs. Ferroelectric materials are known to possess anomalously large BEC and sometimes stereochemically active lone pair. Motivated by these considerations, in this work, we investigate the electronic, structural, and vibrational properties of various chloride-based perovskites in cesium-family, using first-principles density-functional theory calculations. The property trends in various aspects such as formability, band gap, Born effective charge (BEC), dielectric constant, and phonon instabilities are also discussed in terms of tolerance or/and octahedral factors.

2 Methodology

All our calculations here are performed using the PWSCF [15] implementation of DFT, with a plane-wave basis set and ultrasoft pseudopotentials [16]. We adopt the exchange-correlation functional of Perdew-Zunger (PZ) [17] for the local-density approximation (LDA) and that of Perdew-Burke-Ernzerhoff (PBE) [18] for the generalized gradient approximation (GGA). The Brillouin zone integration is done on a uniform Monkhorst-Pack grid of 8×8×8/N for N×N×N cell. An electronic smearing parameter of 0.01 Ry with Fermi-Dirac distribution is used. Structural relaxation is carried out in each case so as to minimize the forces acting on each of the atoms using the Broyden-Flecher-Goldfarb-Shanno (BFGS) based method. Phonon frequencies are obtained using the Density Functional Perturbation Theory (DFPT) which calculates full dynamical matrices through the linear response of electrons to a static perturbation induced by the ionic displacements.

3 Results and Discussions

3.1 Structure

First, we report the properties of the high symmetry cubic perovskite structure of the family $CsBCl_3$ with B = Hg, Si, Ge, Sn, Pb, Mg, Ca, Sr, Ba. As our compounds,

are known to be non-magnetic, we perform non spin polarized calculations. In aristotype cubic phase, the atomic positions are fixed by symmetry and the only structural parameter needs to be relaxed is the lattice constant a. Our result is reported in Table 2 and compared with experimental values. Our relaxed lattice constants are in good agreement with the experimental data.

Table 1: Various geometric factors to account for property trends.

Compound	Group of B atom	Tolerance factor t	Octahedral factor $\frac{R_B}{R_X}$	$\frac{R_{Cs}}{R_B}$	Experimental ground state	Cubic T_c (K)	Expt-al Band Gap(eV)	
							cubic	RT
$CsSiCl_3$	IV	1.034	0.359	2.61				
$CsGeCl_3$	IV	1.027 [19]	0.403	2.55	R3m at 298 K	428		3.67
$CsSnCl_3$	IV	0.950	0.608	2.00	$P2_1/n$ at 298 K	390	3.50	4.00
$CsCaCl_3$	II	0.930 [19]	0.552	1.88	P4/mbm at 95 K	95		8.08
$CsSrCl_3$	II	0.874	0.652	1.59	P4mm at 298 K	386		7.62
$CsPbCl_3$	II	0.871 [19]	0.657	1.58	P1 at 176 K	320		3.00
$CsBaCl_3$	II	0.827	0.746	1.39				

Table 2: Theoretical lattice parameter (Å) of cubic phases as obtained from DFT method in comparison to experimental data.

Tolerance factor t	Compound	a_0 (Å)			Band Gap (eV)		
		LDA	PBE	Expt	LDA	PBE	Expt
1.034	$CsSiCl_3$	5.006	5.234		0.1	0.1	
1.027 [19]	$CsGeCl_3$	5.080	5.324	5.475	0.2	1.2	3.67
0.950	$CsSnCl_3$	5.404	5.641		0.3	1.1	3.50
0.930 [19]	$CsCaCl_3$	5.281	5.487	5.382	6.1	5.5	8.08
0.874	$CsSrCl_3$	5.503	5.720	5.605	5.5	5.1	7.62
0.871 [19]	$CsPbCl_3$	5.514	5.731	5.605	1.6	2.4	3.00
0.827	$CsBaCl_3$	5.821	5.969		4.3	4.9	

Our DFT calculations (see Table 2) show that the above cubic chloro-perovskite structures remain insulator for all B cations that we have explored here, however at the DFT level the values are expected to underestimate the experimental bandgap as usual.

Table 3: Born effective charges (e) and electronic dielectric tensor of cubic $CsBCl_3$ (at the LDA volumes). The nominal charge of corresponding ions (e) are +1, +2, and -1 for Cs, B and Cl ions respectively.

		Z^*_{Cs}		Z^*_B		$Z^*_{Cl_\parallel}$		$Z^*_{Cl_\perp}$		ϵ^∞	
t	Compound	LDA	PBE	LDA	PBE	LDA	PBE	LDA	PBE	LDA	PBE
1.034	$CsSiCl_3$	1.33	1.32	6.00	5.59	-5.31	-5.40	-0.85	-0.68	8.919	7.143
1.027 [19]	$CsGeCl_3$	1.31	1.31	5.19	4.79	-4.89	-4.68	-0.73	-0.69	6.697	5.227
0.950	$CsSnCl_3$	1.31	1.44	4.53	4.17	-4.70	-4.39	-0.62	-0.65	6.048	4.657
0.930 [19]	$CsCaCl_3$	1.30	1.70	2.39	2.45	-1.89	-1.93	-0.90	-0.92	2.871	2.681
0.874	$CsSrCl_3$	1.30	1.29	2.41	2.42	-1.91	-1.89	-0.90	-0.91	2.711	2.479
0.871 [19]	$CsPbCl_3$	1.29	1.34	4.04	3.86	-3.93	-3.65	-0.70	-0.75	4.306	3.68
0.827	$CsBaCl_3$	1.29	1.44	2.57	2.58	-2.10	-2.10	-0.88	-0.89	2.598	2.440

Table 4: Calculated (including LO-TO splitting) lowest phonon frequencies (in cm^{-1}) of cubic structures at calculated equilibrium LDA lattice constants for high symmetry q-points.

		Group	Γ		R		M		X	
Tolerance	Compound	of B	LDA	PBE	LDA	PBE	LDA	PBE	LDA	PBE
1.034	$CsSiCl_3$	IV	$197i$	$(241i)$	56	(49)	$168i$	$(225i)$	$182i$	$(232i)$
1.027 [19]	$CsGeCl_3$	IV	$80i$	$(135i)$	51	(44)	$61i$	$(112i)$	$70i$	$(121i)$
0.950	$CsSnCl_3$	IV	24	(19)	$40i$	(10)	$43i$	(13)	21	(29)
0.930 [19]	$CsCaCl_3$	II	46	(77)	$35i$	(31)	$35i$	(31)	34	(59)
0.874	$CsSrCl_3$	II	$21i$	(15)	$57i$	$(29i)$	$57i$	$(27i)$	$14i$	(13)
0.871 [19]	$CsPbCl_3$	II	$22i$	(46)	$53i$	$(36i)$	$55i$	$(35i)$	$14i$	(37)
0.827	$CsBaCl_3$	II	$54i$	(36)	$67i$	$(44i)$	$68i$	$(43i)$	$50i$	(23)

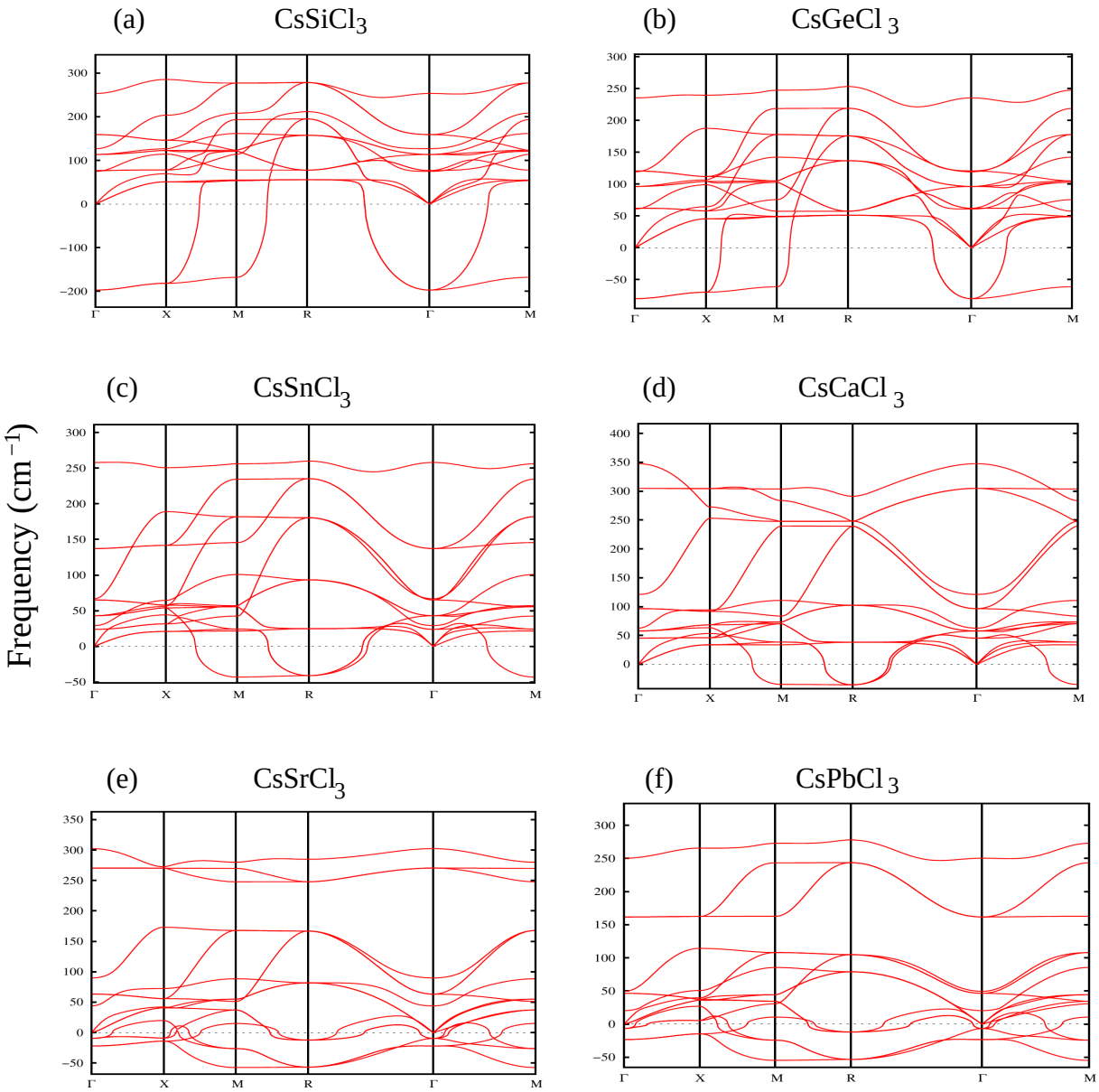

Figure 5: Phonon dispersion Curves.

3.2 Dielectric properties

Knowledge of the Born effective charges (Z^*) and the optical dielectric tensor (ϵ_∞) is essential for describing the long-range dipolar contribution to the lattice dynamics of a polar insulator. In Table 3 we report Z^* and ϵ_∞ of cubic $CsBCl_3$. In the cubic structure, Z^* of Cs and B are isotropic while, for Cl, two distinct values are considered depending if the Cl atom is displaced along the B−Cl chain ($Cl_\parallel$) or perpendicularly to it ($Cl_\perp$). The Born effective charges of Si (+6.00 e) and $Cl_\parallel$ (-5.31 e) in $CsSiCl_3$; and of Ge (+5.19 e) and $Cl_\parallel$ (-4.89 e) in $CsGeCl_3$ are strongly anomalous, when the nominal charges are +2 e for Si, Ge and -1 e for Cl. These anomalous Born effective charges are a common feature of ABX_3 compounds and are related to the covalent character of the B-X bond[?]. Z^*_{Sn} and $Z^*_{Cl_\perp}$ in $CsSnCl_3$; and Z^*_{Pb} and $Z^*_{Cl_\perp}$ in $CsPbCl_3$ are also anomalous but to relatively lower extent. For the rest, the Born effective charges are anomalous but to a much lower extent. As illustrated in Tab. 3, the Z^* of $CsBCl_3$ with column IV elements at B sites are much larger than to those of $CsBCl_3$ with column II elements at B sites, consistent with the fact that the covalent character are much larger for the former than for the latter. The calculated optical dielectric constants are of 8.919 for $CsSiCl_3$ and 6.697 for $CsGeCl_3$. They are much larger than for $CsBaCl_3$, coherently with the larger bandgap of $CsBaCl_3$. Furthermore, in Figure 3, we render the charge-density plot in the (111) plane.

3.3 Phonon Dispersions

In Figure 4, we report the phonon dispersion curves of cubic $CsBCl_3$. The ΓX, ΓM, and ΓR lines are along the [100], [110], and [111] directions, respectively. Negative values in the graph correspond to imaginary phonon frequencies that relate to unstable modes. As seen in the above figures, in most of the compounds, there are strong AFD instabilities at the R point and at the M point corresponding to rotations of oxygen octahedra ($a^0a^0c^-$ at R and $a^0a^0c^+$ at M, following the Glazer's notation [12]). Interestingly, we do also observe a FE instability at Γ in $CsBaCl_3$, $CsGeCl_3$, and $CsSiCl_3$. The Γ instability is a TO mode that involve the polar motion of B and Cl atoms.

For the high values of t ($t > 1$), we find ferroelectric instability (FE) which is of B type; whereas for the low values of t ($t \leq 0.877$), antiferrodistortive (AFD) instability exists along with FE instability of A type, but AFD is usually stronger. In the intermediate range ($0.877 < t < 0.950$), we find only AFD instability (in LDA) or very soft AFD mode (in GGA) [see Table 4].

4 Conclusions

In summary, using first-principles density functional theory, we determine the structural, electronic and vibrational properties of various chloride-based perovskites of the family $CsBCl_3$ with B = Eu, Hg, Si, Ge, Sn, Pb, Mg, Ca, Sr, Ba. We start from the high-symmetry cubic phase, for which electronic band structures, charge-density plots, Born effective charges and phonon dispersion curves are reported. In many of these compounds, we find the coexistence of structural antiferrodistortive instabilities at the zone-boundary points and a ferroelectric instability at the zone center. In particular, for $CsEuCl_3$, from the inspection of the unstable modes in the phonon dispersion curves, various possible types of lattice distortions are determined and the energies of the corresponding phases are calculated. Even though, a long time back $CsEuCl_3$ was experimentally reported to be a ferroelectric material, we here find that the strong antiferrodistortive motions suppress ferroelectricity and are responsible for a non-polar orthorhombic ground state. We nevertheless find that some members of the family such as $CsSiCl_3$ or $CsGeCl_3$ exhibit giant anomalous Born effective charges and phonon dispersion curves similar to $BaTiO_3$ and display a ferroelectric ground state. The tendency to ferroelectricity in terms of the type and size of the B cation is discussed.

Bibliography

[1] K. M. Rabe and Ph. Ghosez. First-principles study of Ferroelectric oxides. *in Physics of Ferroelectrics*, Ed. By K. M. Rabe, C. H. Ahn and J.-M. Triscone; Topics in Applied Physics 105, 111-166 (2007).

[2] W. Zhong, David Vanderbilt, and K. M. Rabe. Phase Transitions in BaTiO3 from First Principles, *Phys. Rev. Lett.* 73, 1861 (1994).

[3] P. Souvatzis, O. Eriksson, M. I. Katsnelson and S.P. Rudin. Entropy driven stabilization of energetically unstal crystal structures explained from first-principles theory, *Phys. Rev. Lett.* 100, 095901 (2008).

[4] H. Olijnyk and W.B. Holzapfel. Phase transitions in alkaline earth metals under pressure. *Phys. Lett.*, 100A, 1984.

[5] Hiroshi Fujihisa, Yuki Nakamoto, Katsuya Shimizu, Takahiro Yabuuchi, and Yoshito Gotoh. Crystal structures of calcium iv and v under high pressure. *Phys. Rev. Lett.*, 101:095503, Aug 2008.

[6] W.L. Mao, Lin Wang, Y. Ding, W. Yang, W. Liu, D. Y. Kim, W. Luo, R. Ahuja, Y. Meng, S. Sinogeikin, J. Shu, and H. Mao. Distortions and stabilization of simple-cubic calcium at high pressure and low temperature. *Proc. Natl. Acad. Sci. U.S.A.*, 107, 2010.

[7] J. S. Tse, S. Desgreniers, Y. Ohishi, and T. Matsuoka. Large amplitude fluxional behaviour of elemental calcium under high pressure. *Scientific Reports*, 2, April 2012.

[8] T. Yabuuchi, Y. Nakamoto, K. Shimizu, and T. Kikegawa. New high-pressure phase of calcium. *J. Phys. Soc. Jpn.*, 74, 2005.

[9] A. M. Teweldeberhan and S. A. Bonev. High-pressure phases of calcium and their finite-temperature phase boundaries. *Phys. Rev. B*, 78:140101, Oct 2008.

[10] Ion Errea, Bruno Rousseau, and Aitor Bergara. Anharmonic stabilization of the high-pressure simple cubic phase of calcium. *Phys. Rev. Lett.*, 106:165501, Apr 2011.

[11] Yansun Yao, Dennis D. Klug, Jian Sun, and Roman Martoňák. Structural prediction and phase transformation mechanisms in calcium at high pressure. *Phys. Rev. Lett.*, 103:055503, Jul 2009.

[12] A.M. Glazer, Acta Cryst. B **28**, 3384 (1972).

[13] Ph. Ghosez, E. Cockayne, U. V. Waghmare and K. M. Rabe, Phys. Rev. B **60**, 836 (1999).

[14] Sinisa Coh et al. Phys. Rev. B **82**, 064101 (2010).

[15] S. Baroni, S. de Gironcoli, A. Dal Corso and P. Giannozzi, http://www.pwscf.org.

[16] D. Vanderbilt, Phys. Rev. B **41**, 7892 (1990).

[17] J. P. Perdew and A. Zunger, Phys. Rev. B **23**, 5048 (1981).

[18] J. P. Perdew, K. Burke and M. Ernzerhof, Phys. Rev. Lett. **77**, 3865 (1996).

[19] R. L. Moreira and Anderson Dias, J. Phys. Chem. Solids **68** 1617 (2007).

[20] A.N. Christensen and S.E. Rasmussen, Acta. Chem. Scand. **19** 421 (1965).

[21] M. C. Marco de Lucas et al., J. Phys. Chem. Solids **56** 995 (1995).

[22] Rick Ubic, J. Am. Ceram. Soc. **90**, 3326 (2007).

[23] K. Heidrich, et al., Phys. Rev. B **24** 5642 (1981).

[24] D.-K. Seo et al., Inorg. Chem. **37**, 407 (1998).

Scientific output

1 List of workshops and visit

In this period, I attended the following meetings and delivered various presentations with BELSPO support properly advertised (reported in chronological order).

- Workshop on the SCAILD method and similar computational approaches in lattice dynamics, University of Uppsala, Sweden, 27-28 August 27 -28, 2012 (invited talk presented)
  Title of talk : The SCAILD method interfaced with ABINIT and QE : its applications and related issues

- A visit to Max Planck Institute of Microstructure Physics Weinberg 2, 06120 Halle (Saale), Germany, June 26-28 2012 (invited talk presented)
  Title of talk : Structural, electronic and vibrational properties of functional ABX_3 materials using DFT and SCAILD method

- Fourth International OxIDes Workshop: Engineering exotic phenomena at oxide interfaces, Santander, Spain, May 30-June 1 2012 (invited talk presented)
  Title of talk : Anharmonic stabilization of high temperature phase of BaTiO3 using SCAILD method

- Workshop on the Fundamental Physics of Ferroelectrics and Related Materials, Argonne National Laboratory, Argonne, IL, USA, January 29 - February 1, 2012 (poster presented)
  Title of poster : Structural, electronic, and vibrational properties of chloride-based perovskites : A first-principles study

- Third International OxIDes Workshop: Engineering exotic phenomena at oxide interfaces, Olbia, Italy, May 24-28 2011.

- 5th International ABINIT Developer Workshop, Han-sur-Lesse 5580, Belgium, April 11 - 14, 2011 (poster presented)
  Title of poster : The Self-consistent ab-initio Lattice Dynamical Method interfaced with ABINIT and QE

2 List of publications in preparation

- **Srijan Kumar Saha**, and Philippe Ghosez, "Structural, electronic and vibrational properties of chloride-based perovskites : A first-principles study"
- **Srijan Kumar Saha**, and Philippe Ghosez, "Structural, electronic and vibrational properties of $CsEuCl_3$ with and without strain : A first-principles study"
- Marco DiGennaro, **Srijan Kumar Saha**, and M. Verstraete, "Anharmonic stabilization of high-pressure phase of Calcium using SCAILD method"